ADVANCED FUNCTIONAL MATERIALS
www.afm-journal.de

Spontaneous Directional Self-Cleaning on the Feathers of the Aquatic Bird *Anser cygnoides domesticus* Induced by a Transient Superhydrophilicity

Kang Luan, Meijin He, Bojie Xu, Pengwei Wang, Jiajia Zhou, Binbin Hu, Lei Jiang, and Huan Liu**

In nature, the feathers of the goose *Anser cygnoides domesticus* stay superhydrophobic over a long term, thought as the main reason for keeping the surface clean. However, contaminants, especially those that are oleophilic or trapped within textures, cannot be removed off the superhydrophobic feathers spontaneously. Here, a different self-cleaning strategy based on superhydrophilic feathers is revealed that is imparted by self-coating of the amphiphilic saliva, which enables removing away low-surface-tension and/or small-size contaminants by forming directional water sheeting depending on their unique anisotropic microstructures. Particularly, the surface superhydrophilicity is switchable to superhydrophobicity upon exposure to air for maintaining a clean surface for a long time, which is further enhanced by coating with self-secreted preening oil. By alternate switching between a transient superhydrophilicity and a long-term stable superhydrophobicity, the goose feathers exhibit an integrated smart self-cleaning strategy, which is also shared by other aquatic birds. An attractive point is the re-entrant structure of the feathers, which facilitates not only liquid spreading on superhydrophilic feathers, but also long-term stability of the cleaned surface by shedding water droplets off the superhydrophobicity feathers. Thus, artificial self-cleaning microtextures are developed. The result renews the common knowledge on the self-cleaning of aquatic bird feathers, offering inspiration for developing bioinspired self-cleaning microtextures and coatings.

1. Introduction

In nature, self-cleaning is an unique ability shared by many organisms, especially those living in the highly humid environment, which are mostly imparted by the superhydrophobic surfaces.[1] For example, lotus leaves keep long time cleaning despite living in a pond with silt; mosquito eyes stay self-cleaning against moisture; self-cleaning cicada wings contribute to the long-time maintaining of its antireflection nature.[1] Water droplets easily roll off the superhydrophobic surfaces to carry away the dirt particles and other impurities.[1] Drawing inspirations, various artificial self-cleaning surfaces have been developed in the past decade by combining the highly textured roughness and the low surface free energy.[2] Self-cleaning on the superhydrophobic surface enjoys advantages of long-time stability, however, is limited by both the size and the polarity of the dirty particles, and will be severely impaired when dirty particles are able to penetrate into the surface textures and/or damage the surface hydrophobicity.[3] Also, the superhydrophobic surfaces do not warrant self-cleaning and anticontamination capabilities at sub-micrometric length scales.[4] On the other hand, superhydrophilic surfaces are capable of removing away the dirty particles either trapped within textures or with low surface energy by forming the water sheeting.[5] For example, the fish skin keeps from being contaminated by oils underwater.[5d] The notable drawback for the self-cleaning superhydrophilicity surface is its poor stability as it can be easily contaminated. Thus, it is desirable for a self-cleaning surface to bear the advantageous of both superhydrophilic and

K. Luan, Dr. M. He, Dr. B. Xu, Dr. P. Wang, Prof. J. Zhou, Prof. L. Jiang, Prof. H. Liu
Key Laboratory of Bio-Inspired Smart Interfacial Science and Technology of Ministry of Education
School of Chemistry
Beijing Advanced Innovation Center for Biomedical Engineering
Beihang University
Beijing 100191, P. R. China
E-mail: liuh@buaa.edu.cn

The ORCID identification number(s) for the author(s) of this article can be found under https://doi.org/10.1002/adfm.202010634.

DOI: 10.1002/adfm.202010634

K. Luan, Prof. B. Hu
Key Laboratory for Special Functional Materials of Ministry of Education
National & Local Joint Engineering Research Center for High-efficiency Display and Lighting Technology
School of Materials Science and Engineering
Collaborative Innovation Center of Nano Functional Materials and Applications
Henan University
Kaifeng 475001, P. R. China
E-mail: hbb@henu.edu.cn

Prof. L. Jiang
CAS Key Laboratory of Bio-inspired Materials and Interfacial Science
Technical Institute of Physics and Chemistry
Chinese Academy of Sciences
Beijing 100190, P. R. China

superhydrophobic surfaces mentioned above, which remains unsolved so far.

For a long time, the superhydrophobic feathers of the goose, aroused by its highly textured structures and the self-repairable surface coating of the preening oil, have been considered as the main reason for keeping feathers clean.[6,7] However, contaminants, especially oleophilic ones or those with small size that can be trapped within textures, cannot be removed off the superhydrophobic feathers spontaneously. Here, we revealed a smart superhydrophilicity induced self-cleaning strategy of the goose feathers, which proceeds spontaneously and directionally to remove away both oleophilic and small size contaminants. The surface superhydrophilicity, imparted by self-coating of the amphiphilic saliva, is responsible for a complete self-cleaning by forming the water sheeting. Upon exposing in air, the feather turns into a superhydrophobic state to maintain a long time durability of the cleaned surface by shedding off water droplets. Notably, liquids on the anisotropic structured feathers are liable to transport directionally, based on which various kinds of contaminants can be expelled away in a preferred direction. We also demonstrated that such spontaneous directional self-cleaning is applicable to feathers of other aquatic birds and bioinspired artificial surfaces.

2. Results and Discussion

Combing feather using bill is a frequent motion for the aquatic bird such as the goose (*Anser cygnoides domesticus*) (**Figure 1**a), by which process not only the messed feathers can be adjusted into the ordered structures for repairing the tear resistance,[8] but also the self-secreted preening oils (Figure 1a, the left inset) are coated on the feather for maintaining the long-term stable superhydrophobicity (Figure 1b).[6] In case the surface lipids were damaged, the superhydrophobicity of the feather would be impaired, and can be recovered by artificial coating a thin layer of the preening oil, as has been confirmed experimentally (Figure S1, Supporting Information). Besides the preening oils, the saliva, another important secretion of the aquatic bird, is also able to be coated on the feathers during combing feathers, which however has been neglected for a long time.

We demonstrated that the saliva (Figure 1a, the right inset) is capable of altering the surface wettability drastically into a superhydrophilic state by forming the surface coating when the goose comb feather using bill (Figure 1c, 3.96 s). The saliva is a typical liquid mixture containing large amount of water and small amount of proteins. The proteins have both hydrophobic and hydrophilic amino acid side chains,[9] thus they can work as surfactants to facilitate the water spreading on the superhydrophobic feather. The hydrophobic amino acid side chains are liable to be adsorbed on the hydrophobic feather, leaving hydrophilic amino acid chains exposed to air.[9b] By self-coating the saliva during combing feathers, the feather shows superhydrophilicity (Figure 1c, 3.96 s), which is transient and can gradually turn back to the superhydrophobic state when exposed to air (Figure 1c, 118 min). Such superhydrophobicity of the feather is self-repairable with a good durability in air, which is attributable to the self-coating of the preening oil.[6] As shown in Figure 1d, a single feather on goose wings is about 15–20 cm in length, composing a main shaft (rachis and calamus) and a vane in which feather barbs branch from the shaft.[8,10] The single feather barb is ≈4–5 cm in length and ≈800 μm in width (Figure 1e), showing a typical asymmetric microstructure on both sides. Notably, the water transport directionally on the superhydrophilic feather from the shaft side to the edge side in a preferred direction *B*, while was pinned in the opposite direction *A* (Figure 1f; Movie S1, Supporting Information). Such directional liquid transport on the superhydrophilic feather leads to a desirable directional self-cleaning behavior, by which containments including low-surface-tension liquids, small particles trapped within textures, and sub-micrometric liquid droplets can be expelled away from the feather (Figure 1g). These contaminants are difficult to be removed from the superhydrophobic feathers (Figure 1h), as has been revealed very recently.[3,4] The superhydrophobic state of the feathers also contribute to the removing contaminants of big size, but more importantly it is responsible for the long-time maintaining of the surface clean (Figure 1h). Therefore, by alternate utilizing both a transient superhydrophilicity and long-term stable superhydrophobicity, the goose feathers show a rather smart self-cleaning strategy.

The directional self-cleaning behavior on the superhydrophilic goose feather was in situ visualized by the directional expulsion away of the pre-spread silicone oil contaminants using directional water flow. By staining the water and silicone oil with Rhodamine B (dark-red-color) and Coumarin 6 (light-green-color), respectively, the trace of liquid transport was visualized by both the optical (**Figure 2**a) and the fluorescence (Figure 2b; Movie S2, Supporting Information) microscopes. At the beginning, the superhydrophilic feather was partially contaminated by the silicone oil (Figure 2a,b, 0 s). Upon dropping on the dry area, water would immediately transport directionally along direction *B* (Figure 2a, 0.44 s, Figure 2b, 0.52 s). Once the front edge of the water film (blue arrow) met with the edge of the oil (yellow arrow), the water would propel the oil moving directionally, and consequently remove the silicone oil away the feather from the open-end (Figure 2a, 17.28 s, Figure 2b, 3.12 s). Moreover, theoretical analysis based on the minimization of the system's free energy were conducted. Here, the total interfacial energies of feather that are completely wetted by either the low-surface-tension liquid (liquid A) of silicone oil (E_A) or the high-surface-tension liquid (liquid B) of water (E_B) were calculated (Figure 2c). Considering that the feather was preferentially wetted by water, $\Delta E = E_A - E_B = \mathrm{R}(\gamma_\mathrm{B}\cos\theta_\mathrm{B} - \gamma_\mathrm{A}\cos\theta_\mathrm{A}) + \gamma_\mathrm{A} - \gamma_\mathrm{B}$ must be greater than zero (Supplementary text 1). It suggested that the replacement of oils by water on the superhydrophilic feather is an energy favorable process.[11] Taken together, we revealed a superhydrophilicity-induced directional self-cleaning strategy on the goose feather.

To explore the liquid transport behavior on the fibrous feather, the microstructure of the feather was characterized in detail. As shown, the feather vane was composed of numerous over-lapped feather barbs, and each barb is composed of both grooved barbules and hooked barbules (**Figure 3**a), as has been reported.[8,10,12] Considering the similar liquid transport behavior shared on both grooved and hooked barbules, as well as the similar structure, here we focused on the grooved barbules which is ≈275 μm in width. The grooved barbules

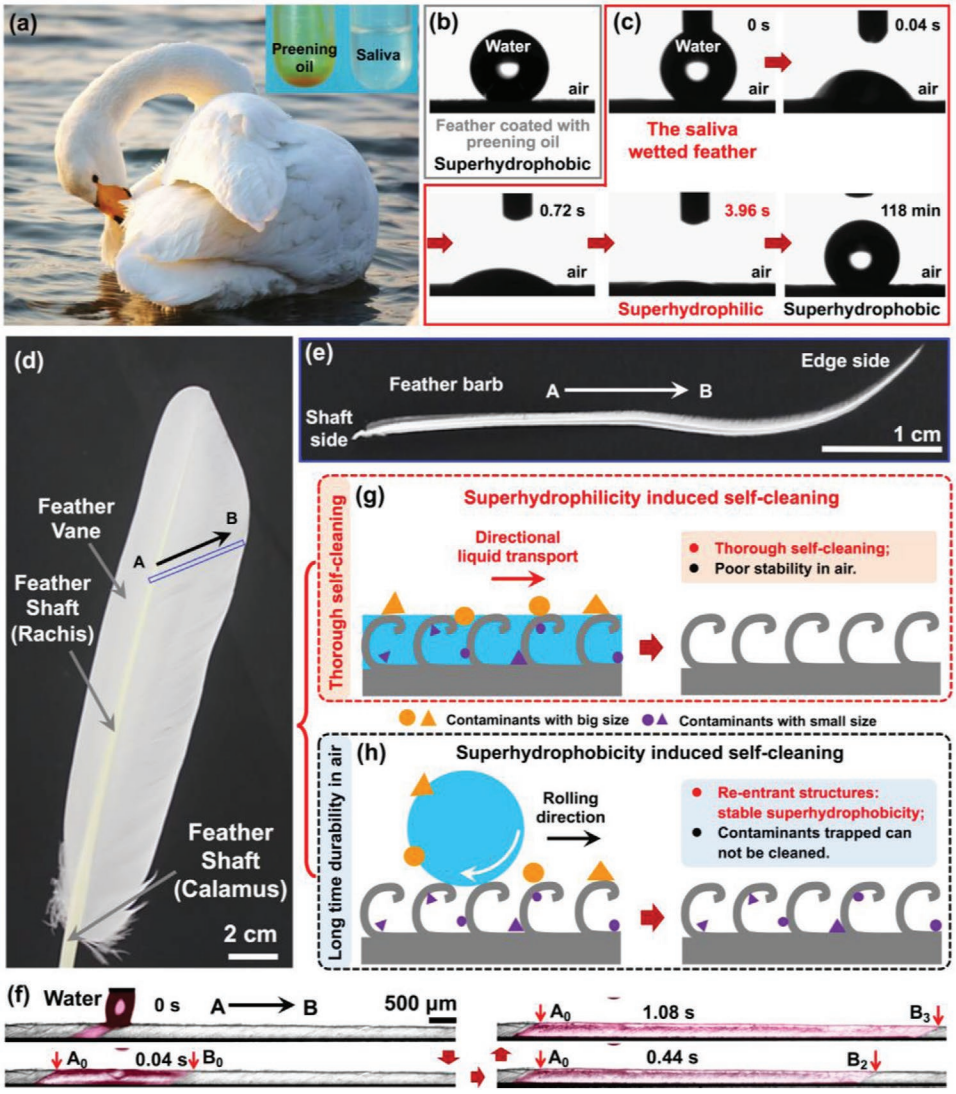

Figure 1. The transient superhydrophilic feather of the goose (*Anser cygnoides domesticus*) imparted by surface coating of its saliva, and the as-generated directional self-cleaning strategy. a,b) The goose feather stay long-time superhydrophobic due to the highly textured structures and the surface coating of the self-secreted preening oil (inset). c) By coating its saliva during combing feathers, the feather shows a superhydrophilic state, then gradually turns back to the original superhydrophobic state upon exposing to air. The optical picture of d) a single goose feather with a length of ≈20 cm, and e) a single feather barb with the length ≈4.5 cm and the width of ≈800 μm. f) The directional liquid transport of water (0.2 μl) on a single feather barb with a preferred direction *B*. g) The schematic cartoon of self-cleaning on a superhydrophilic surface, which is capable of removing contaminants both oleophilic or trapped within textures. h) The schematic cartoon of self-cleaning on a superhydrophobic surface, which is stable in air but unable to remove particles trapped within textures.

show curved laminas structures with dorsally curved margins, forming a typical half-closed concave-shaped microchannels with width of ≈20 μm by overlapping with the neighboring barbules (Figure 3b). Typically, there are two kinds of wedge-like structures in each microchannel: a half meniscus wedge-like corner with a constant angle α of ≈10° at the overlapping part between two neighboring burbles (Figure 3c); a 3D-gradient wedge-like corner with a changeable angle β depending on the local position between the barb and the burble (Figure 3d,e). X-ray microcomputed tomography (Micro-XCT) characterization directly shown the cross sections of the angle β at different position, and the value increased gradually from ≈0°, 11°, 14°, 21° to 29° in direction *B*, corresponding to the position 1, 2, 3, 4, and 5 in Figure 3e (Figure 3d_1–d_5; Movie S3, Supporting Information). To be noticed, the α is located beneath the β and the distance Δh decreases with the increase of value of β (Figure 3d_1–d_5). Particularly, liquid transport on the superhydrophilic feather prefers the direction from the small angle side to the big angle side along a gradient corner β, which is a rather smart design for easy removing away the contaminant (Figure 3e). Such directional liquid transport differs from that on the peristome surface of *Nepenthes alata*, where liquid is liable to transport to the closing-side of the wedge.[13] To be noticed, the re-entrant structural nature of the feather, characterized by the curved margin of each individual barbule (Figure 3f), facilitate both the liquid spreading on the

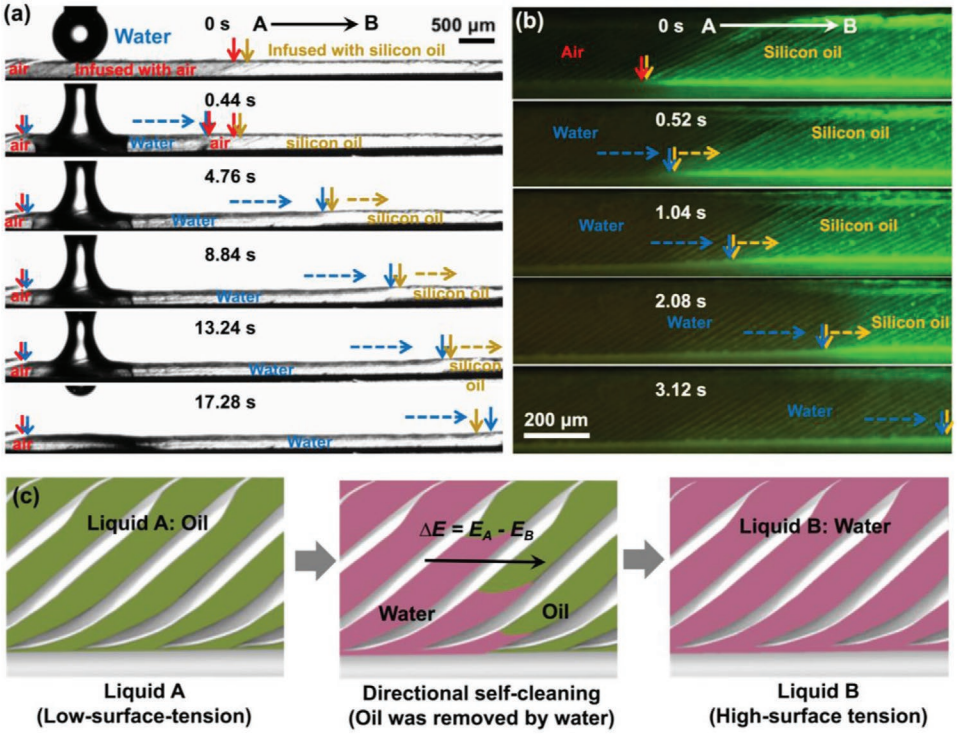

Figure 2. Directional self-cleaning behavior on the superhydrophilic feather of the goose (*Anser cygnoides domesticus*). a,b) The dynamic process of the directional self-cleaning where the water can easily drive away the spread oil with a preferred direction *B*, observed by the a) optical and b) fluorescence microscope. The water and silicone oil were colored with Rhodamine B and Coumarin 6, respectively. c) The schematic cartoon and the theoretical analysis based on the minimization of a system's free energy, indicating an energy favorable process of the spontaneous self-cleaning process.

superhydrophilic feathers[14] and the water droplets shedding off the superhydrophobicity feathers.[15] As schematically shown in Figure 3g, the unique two-level anisotropic microstructures of the feather was characterized by the alternate wedge α and β along the feather barb, by which the directional liquid transport proceeds programmably with reaching to each corners and being drained off finally. Here, the optimized short-distance liquid transport along the 3D-gradient wedge β determines the direction; while the long-distance liquid transport was enabled by the wedge α.

The directional liquid transport is the key for the directional self-cleaning behavior, and its dynamic process on the feather was *in-situ* characterized using a high speed CCD. As shown, upon being dropped on fibrous feather, liquid will immediately transport in a preferred direction *B*, while being pinned in direction *A* (**Figure 4**a). In direction *A*, liquid can hardly enter the next microchannel after it fills the microchannel where the liquid was released (Figure 4b), which is attributable to the edge-pinning effect at one end of the angle β (Figure 4c) according to the Gibbs inequality.[16] Such edge-pining can be directly confirmed by visualizing the tri-phase contact lines upon solidifying the polydimethylsiloxane (PDMS, Figure 4d). In direction *B*, ultrafast liquid transport was observed (Figure 4e–h). Specifically, the liquid first transport within certain microchannel along a preferred direction (the dashed black arrow, Figure 4h, with the trace from point 1 to 1′, 1″ and then 1‴ (write arrows, Figure 4h, from point 2 to 2′, and 2″ (green arrows, Figure 4h, which is attributable to the capillary rise imparted by the corner effect[17] along the wedge α. When the microchannel was filled to an extent that its liquid level exceeds the top of the tiny opening end of the angle β, liquid will enter into the next microchannel in direction *B*, i.e., point 2 (Figure 4e–h), since the position of the angle α is below the tiny opening end of the angle β. Here, the velocity of water transport within each microchannel (V_1, ≈10.02 mm s^{-1}) is about 4 times faster than that across the microchannel (V_2, ≈2.53 mm s^{-1}), which is attributable to a clearly longer L_2 along the angle α (10°) comparing with L_2 along the angle β. A rather long spreading precursor film was clearly observed along the corner α in the concave shaped microchannel (Figure 4f), which is favorable for the liquid transport.[18] By repeating this process, long-distance directional water transport was enabled on the feathers, which leads to the directional self-cleaning. Particularly, the typical concave-shaped re-entrant structures of the feathers further facilitates liquid spreading on it, which means the liquid spreading on the re-entrant surface is liable to be driven away by another liquid. Moreover, such directional self-cleaning proceed only on the anisotropic structured feathers, but not on the smooth superhydrophilic surface (Figure S2, Supporting Information), which is attributable to the ability of the directional flow in removing contaminants out of the targeted substrate horizontally. With no preferred direction, water and oil would merge together and form bilayer liquids on the smooth surface, with no oil expulsion off the substrate in-plane (Figure S2, Supporting Information). Therefore, both transient superhydrophilicity and anisotropic

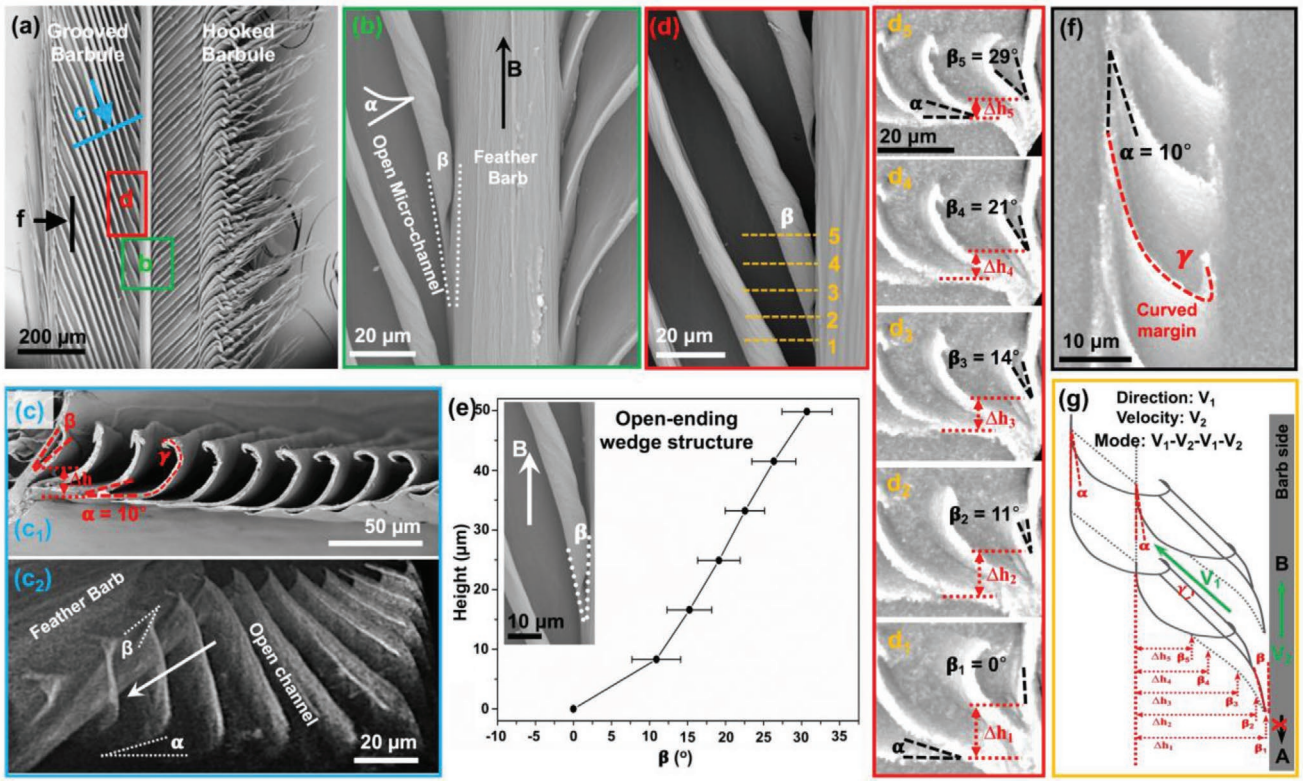

Figure 3. The microstructure of a single feather barb of the goose (*Anser cygnoides domesticus*). a) The feather is composed of the grooved barbules and the hooked barbules, distributing with certain tilt angle to the barb. b) For the grooved barbules, overlapped barbules forms microchannels with a width of ≈20 μm. Two kinds of wedge angles are distinguishable: a half meniscus tiny angle α and gradient wedge angle β. The arrow B indicates the liquid transport direction. c) SEM and Micro-XCT characterization of the cross section of the grooved barbule. d) The angle β increases gradually depending on the position from position 1 to 5. Moreover, the tiny opening end of angle β is always higher than angle α, and the Δh decreases with increasing the angle β. e) The angle β increases gradually from ≈0° to ≈29° in direction *B*. The error bars indicate standard deviations from at least five independent measurements. f) The side-view of the grooved barbule shows the angle α of ≈10° formed by overlapping grooved barbules, where the microchannel is concave shaped with curved margin (red dashed line, γ). g) The schematic cartoon of the microstructures of the grooved barbules.

structure contribute to the directional self-cleaning of the goose feathers.

To further confirm that the unique two-level anisotropic microstructures of the feather is the key for the directional liquid transport, various liquids were investigated on both superhydrophobic and as-treated superhydrophilic feather. As summarize in Table 1 almost all liquids with surface tensions ranging from 9.5 dyn cm^{-1} for FC-72 to 72.8 dyn cm^{-1} for water show clear directional liquid transport behaviors on the superhydrophilic feather. Typically, the transport velocity for liquid of 1, 2-dichloroethane reaches an average value of ≈6.74 mm s^{-1} with an instantaneous fastest velocity up to 23.37 mm s^{-1} (Figure S3, Supporting Information). For the superhydrophobic feathers, only the wettable liquids with the surface tension smaller than 37.70 dyn cm^{-1} can transport. Specifically, the directional transport of the liquid formic acid (surface tension of 37.7 dyn cm^{-1}) was observed only on the as-treated superhydrophilic feather, not on the superhydrophobic feather because of the partial wetting (Figure S4, Supporting Information). Considering the directional self-cleaning behavior of the feather, it was proposed that the directional transport of high surface energy liquid B (water) is capable of propelling liquids with lower surface energy A (oils) moving in a preferred direction.

Inspired by both the superhydrophilicity imparted by the surface coating of its saliva and the unique anisotropic structures of the nature feather, the artificial feather was prepared by 3D printing, whose surface was treated into superhydrophilic with oxygen plasma (**Figure 5**). It clearly shows two typical structural characterizations of the natural feather (Figure 5a): the short microwedge β with a 3D gradient; and the long microwedge α with a fixed small corner (Figure 5b,c). The water on the superhydrophilic artificial feather transport via direction *B* but was almost pinned on the opposite direction (Figure 5d; Movie S4, Supporting Information). When oil droplets (colored into blue) were dispersed on the artificial feather, the subsequent unidirectional water (colored into red) transport can propel the oil off the substrate in a preferred direction, exhibiting a spontaneous directional self-cleaning behavior (Figure 5e; Movie S5, Supporting Information). Particularly, the superhydrophilicity on the bioinspired substrate is hierarchical ordered, attributable to the structural induced programmable capillary rise. Liquid is liable to transport firstly in the micro sub-channels (direction *B′*, Figure 5d, and then move into the next sub-channel in direction *B* (Figure 5d). More importantly, such concept is application for the large-scale fabrication of the artificial self-cleaning microtextures

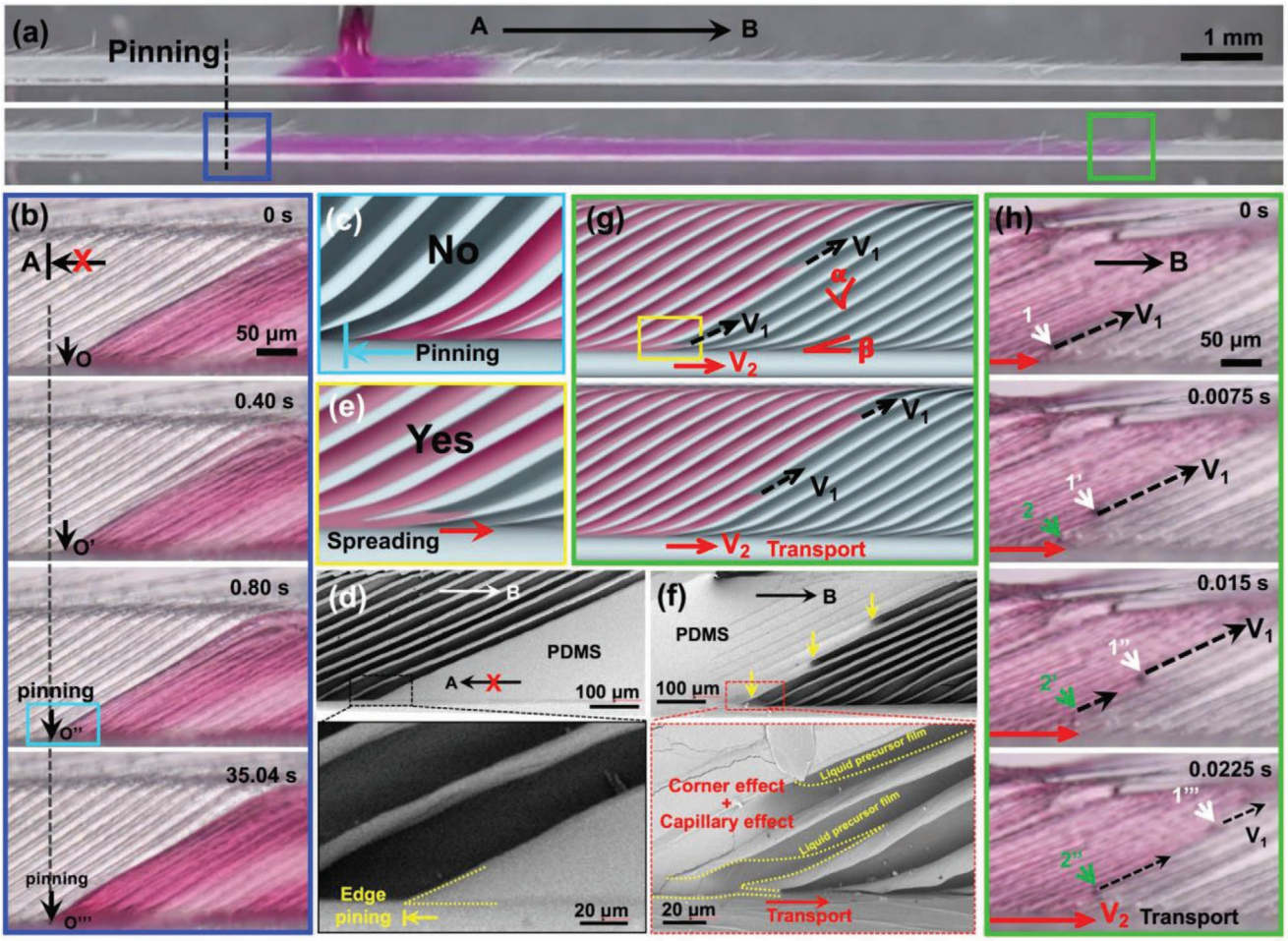

Figure 4. The in situ observation of the directional liquid transport on a single feather. a) Water on the feather transported directionally along direction *B* (the green frame), while was pinned in the opposite direction *A* (the blue frame). b–d) Liquid cannot transport in direction *A* imparted by the edge pinning effect, where the water boundary coinciding with the edge of the small angle side of *β*, as indicated by both c) schematic cartoon and d) the pinning edge on a feather by solidification of PDMS. e–h) Liquid is liable to transport in direction *B*, as indicated by both h) the optical picture and e,g) the schematic cartoons. The moving trace was indicated by the colored arrows 1 and 2 within the same microchannel, respectively. Liquid first transport within the same microchannel at speed V_1, and overflows to generate the upper liquid layer to enter into the next microchannel in direction *B* at speed V_2. Here, $V_1 > V_2$. f) The spreading edge on a feather by solidification of PDMS. The tri-phase contacted line in the microchannels marked with a yellow dotted lines.

Table 1. The directional liquid transport behavior of various liquids with different surface tension: "○" indicates the feasible directional liquid transport and "×" means no directional liquid transport.

Liquid	Surface tension [dyn cm^{-1}]	Directional liquid transport	
		Superhydrophobic feather	As-treated superhydrophilic feather
Perfluorohexane (FC-72)	9.5	○	○
Octane	21.6	○	○
Acetone	24.02	○	○
Acetonitrile	27.2	○	○
1,2-Dichloromethane	32.6	○	○
Formic acid	37.7	×	○
Dimethyl sulfoxide	43.6	×	○
Ethanediol	48.4	×	○
Formamide	57.4	×	○
Glycerin	63.3	×	○
Water	72.8	×	○

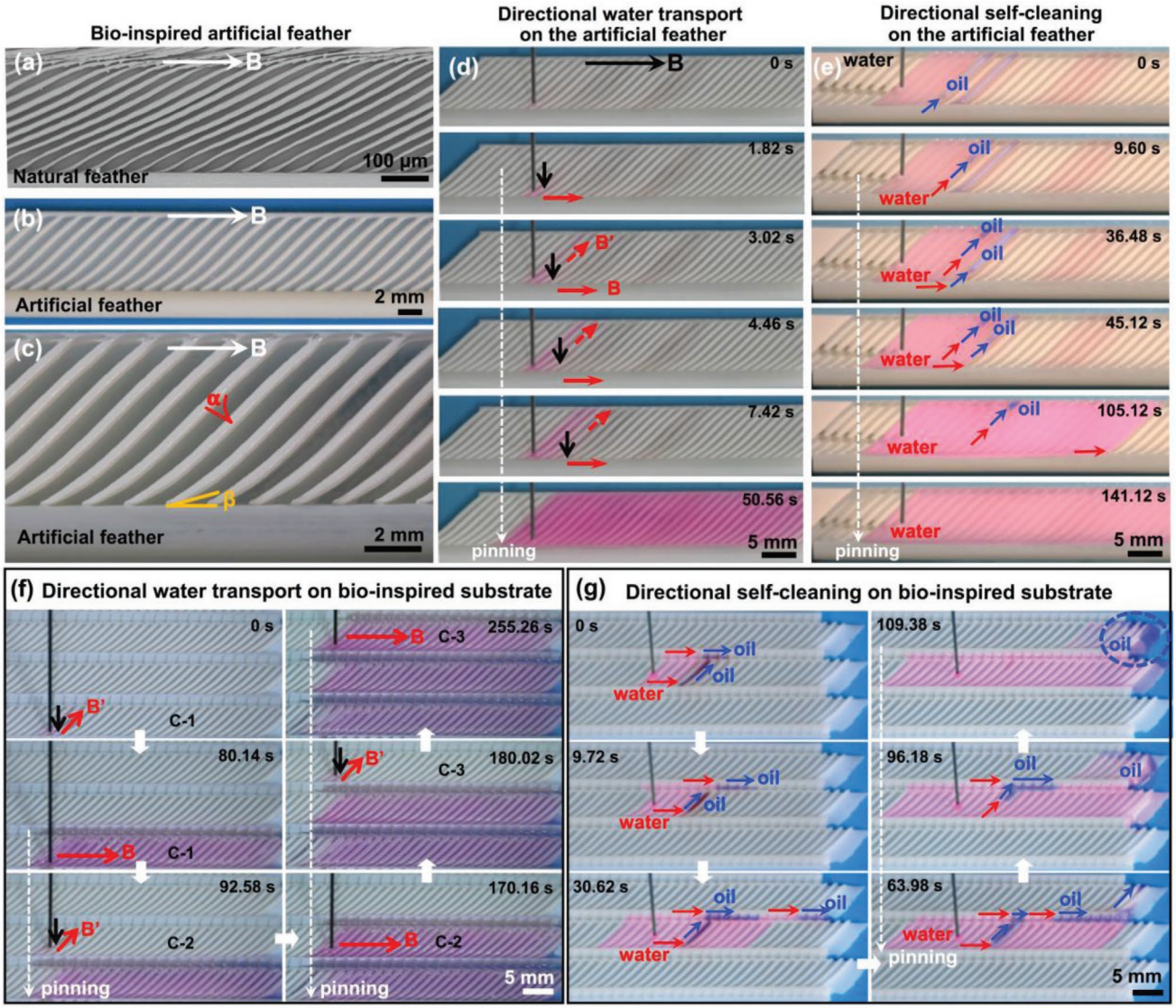

Figure 5. The bioinspired artificial feather shows typical spontaneous directional self-cleaning behavior. *B* indicates the preferred direction for liquids transport. a) SEM image of a natural goose feather. b,c) SEM images of the bioinspired artificial feather with different magnification, showing the similar anisotropic microstructures with that of the nature goose feather. d) The directional water transport on the artificial feather. e) The directional self-cleaning on the artificial feather, where the oil contaminants (colored into blue) was driven away from the substrate in a preferred direction by directional water flow, as indicated by the blue arrows. f) The directional water liquid transport on the bioinspired large-scale substrate. g) The directional self-cleaning on the bioinspired substrate. As a consequence of the directional water transport (red color), the pre-released oil (blue color) was driven away directionally off the substrate, as indicated by the blue arrows.

and coatings, by duplicating the feather structure in a substrate orderly. As shown, the water is liable to transport within each feather-like millimeter scale channel (e.g., C-1, -2, -3, -4, and -5, Figure 5f, depending on the location of water releasing, consequently reaching each corners within the channel in a preferred direction. Of note is that the oil contaminants can be driven away from the substrate even it was released on the center area. As a consequence of the directional transport of water (red color), the pre-released oil (blue color) was driven away directionally off the substrate (indicated by blue arrows in Figure 5g, showing typical spontaneous directional self-cleaning behavior. Thus, we demonstrated that the concept is applicable for developing artificial self-cleaning materials by using technique of 3D printing, which inspires innovative directional self-cleaning microtextures and coatings.

3. Conclusion

In conclusion, we reveal that the feathers of the aquatic bird *Anser cygnoides domesticus* bear strategy of directional self-cleaning by taking advantageous of both the unique transient superhydrophilicity imparted by the surface coating of its saliva and the unique open-ended anisotropic structures. Consequently, the contaminant oils can be driven away by water in a preferred direction, which differs from the general thinking on

self-cleaning of a superhydrophobic feather. The feather demonstrates a delicate fibrous system that is characterized by the periodically alternate two-level of anisotropic microscale wedge structures. The asymmetrical angle β control the direction and the angle α carry the liquid transport over a long distance. By the periodically alternate repeating of two kinds of capillary rise with different effective length, wetting liquids are capable of transport directionally on both biological feathers and bioinspired artificial fibers. We also confirmed that the directional liquid transport was also observed on both the hooked barbules of the goose feather (Figures S5 and S6 and Movie S6, Supporting Information) and feathers of the swan *Cygnus cygnus* and the egret *Egretta garzetta garzetta* (Figure S7, Supporting Information), since they share the similar two-level anisotropic microstructures. We envision that such programmable capillary rises will offer a new concept for developing self-cleaning microtextures and coatings with diverse controllable liquid transport behaviors.

4. Experimental Section

Sample Preparation: The natural goose feathers were collected from the goose (*Anser cygnoides domesticus*) which are commercially available in Beijing China. The feathers of the swan *Cygnus cygnus* and the egret *Egretta garzetta garzetta* were collected in the Zhengzhou Zoo (China). The feathers were cleaned by alcohol and acetone in ultrasonic cleaning instrument in sequence before use. The liquids used including octane, acetone, acetonitrile, 1. 2-dichloroethane, formic acid, dimethyl sulfoxide, ethylene glycol, formamide, and glycerol were from Beijing Chemical works, and the perfluorohexane (FC-72) was from the 3M company.

Removing of the Lipids from the Feather Surface and Recoating of the Preening Oil: The alkaline solution (pH = 12.65) was prepared using sodium hydroxide, heat to 70 °C. The goose feathers was immersed into the solution for 4 h, then was rinsed with alcohol for surface cleaning. By such treatment, the surface lipids was removed, resulting a drastic decreasing of the water CA. The preening oil collected from the goose (*Anser cygnoides domesticus*) was then coated onto the feathers, which leads to the increasing of the water CA on the feathers.

The Observation of the Unidirectional Liquid Transport: The directional liquid transport on natural fibrous feather was observed and recorded by the contact-angle system (Dataphysics OCA25, Germany), camera (Canon 750D, Japan), and optical microscopy (Olympus. BX 53, Japan). For visualized the process, the Rhodamine B was added in the liquid as dying.

Characterization: Scanning electron microscopy (Desktop scanning electron microscopy, Phenom Pro, Holland) was used to characterize the surface microstructures at an accelerating voltage of 5–10 kV. The sample stages were adjusted by tilt angles ranging from 0° to 90° for 3D observation. High-resolution X-ray microcomputed tomography (Micro-XCT 200 Zeiss) was used to investigate the spatial structure of the feathers. The test parameter is voltage of 80 kV, power of 7 kW, exposure time of 10 s, the whole test process at room temperature and atmospheric pressure.

Fabrication of Artificial Feather: The artificial feather with a dimension of 20 mm × 200 mm was designed by 3Ds Max Software (Autodesk). The width of the channels is ≈800 µm. The long microwedge α and the short microwedge β was the same as that of the natural goose feather. Then the artificial feather was printed using commercially available VisiJet M3 Crystal material- a photocurable dielectric resin on ProJet 3510 HD 3D printer. The printing process was performed at a resolution of 25 µm. Then the as-printed parts were developed in ethanol for 5 min to remove uncured resin. Irradiation under a UV light with a wavelength of 315 nm for 10 minutes at room temperature was conducted to increase the mechanical strength of the artificial feather.

Supporting Information

Supporting Information is available from the Wiley Online Library or from the author.

Acknowledgements

K.L. and M.H. contributed equally to this work. This work was financially supported by the National Key R&D Program of China (2018YFA0704801) and the National Natural Science Foundation of China (21872002).

Conflict of Interest

The authors declare no conflict of interest.

Data Availability Statement

Research data are not shared.

Keywords

bioinspired artificial feathers, directional self-cleaning, fibrous feathers, liquid transport, superhydrophilicity

Received: January 12, 2021
Revised: March 24, 2021
Published online: April 18, 2021

[1] a) W. Barthlott, C. Neinhuis, *Planta* **1997**, *202*, 1; b) R. Blossey, *Nat. Mater.* **2003**, *2*, 301; c) M. Liu, S. Wang, L. Jiang, *Nat. Rev. Mater.* **2017**, *2*, 17036; d) S. Wang, K. Liu, X. Yao, L. Jiang, *Chem. Rev.* **2015**, *115*, 8230.

[2] a) D. Wang, Q. Sun, M. J. Hokkanen, C. Zhang, F. Lin, Q. Liu, S. Zhu, T. Zhou, Q. Chang, B. He, Q. Zhou, L. Chen, Z. Wang, R. H. A. Ras, X. Deng, *Nature* **2020**, *582*, 55; b) X. Deng, L. Mammen, H. Butt, D. Vollmer, *Science* **2012**, *335*, 67; c) X. Tian, T. Verho, R. H. A. Ras, *Science* **2016**, *352*, 142; d) Y. Lu, S. Sathasivam, J. Song, C. R. Crick, C. J. Carmalt, I. P. Parkin, *Science* **2015**, *347*, 1132; e) M. B. Avinash, E. Verheggen, C. Schmuck, T. Govindaraju, *Angew. Chem., Int. Ed.* **2012**, *51*, 10324; f) M. Konar, B. Roy, T. Govindaraju, *Adv. Mater. Interfaces* **2020**, *7*, 2000246.

[3] a) F. Geyer, M. D'Acunzi, A. Sharifi-Aghili, A. Saal, N. Gao, A. Kaltbeitzel, T. Sloot, R. Berger, H. Butt, D. Vollmer, *Sci. Adv.* **2020**, *6*, eaaw9727; b) P. Papadopoulos, L. Mammen, X. Deng, D. Vollmer, H. Butt, *Proc. Natl. Acad. Sci. USA* **2013**, *110*, 3254.

[4] W. S. Y. Wong, T. P. Corrales, A. Naga, P. Baumli, A. Kaltbeitzel, M. Kappl, P. Papadopoulos, D. Vollmer, H. Butt, *ACS Nano* **2020**, *14*, 3836.

[5] a) R. Wang, K. Hashimoto, A. Fujishima, M. Chikuni, E. Kojima, A. Kitamura, M. Shimohigoshi, T. Watanabe, *Nature* **1997**, *388*, 431; b) S. Huang, W. Wang, *Angew. Chem., Int. Ed.* **2017**, *56*, 9053; c) C. Shi, B. Yan, L. Xie, L. Zhang, J. Wang, A. Takahara, H. Zeng, *Angew. Chem., Int. Ed.* **2016**, *55*, 15017; d) M. Liu, S. Wang, Z. Wei, Y. Song, L. Jiang, *Adv. Mater.* **2009**, *21*, 665.

[6] a) A. B. D. Cassie, S. Baxter, *Trans. Faraday Soc.* **1944**, *40*, 546; b) A. B. D. Cassie, S. Baxter, *Nature* **1945**, *155*, 21; c) A. Bolliger, D. Varga, *Nature* **1961**, *190*, 1125; d) E. Haahti, K. Lagerspetz,

T. Nikkari, H. M. Fales, *Comp. Biochem. Physiol.* **1964**, *12*, 435; e) A. Salibian, D. Montalti, *Braz. J. Microbiol.* **2009**, *69*, 437.
[7] R. J. Kennedy, *Nature* **1970**, *227*, 736.
[8] F. Zhang, L. Jiang, S. Wang, *Proc. Natl. Acad. Sci. USA* **2018**, *115*, 10046.
[9] a) S. P. Humphrey, R. T. Williamson, *J. Prosthet. Dent.* **2001**, *85*, 162; b) Y. F. Zhang, J. Zheng, L. Zheng, Z. R. Zhou, *J. Mech. Behav. Biomed. Mater.* **2015**, *42*, 257.
[10] T. N. Sullivan, M. Chon, R. Ramachandramoorthy, M. R. Roenbeck, T. Hung, H. D. Espinosa, M. A. Meyers, *Adv. Funct. Mater.* **2017**, *27*, 1702954.
[11] a) T. Wong, S. H. Kang, S. K. Y. Tang, E. J. Smythe, B. D. Hatton, A. Grinthal, J. Aizenberg, *Nature* **2011**, *477*, 443; b) Y. Wang, J. Di, L. Wang, X. Li, N. Wang, B. Wang, Y. Tian, L. Jiang, J. Yu, *Nat. Commun.* **2017**, *8*, 575; c) J. D. Smith, R. Dhiman, S. Anand, E. Reza-Garduno, R. E. Cohen, G. H. McKinley, K. K. Varanasi, *Soft Matter* **2013**, *9*, 1772; d) D. Quéré, *Annu. Rev. Mater. Res.* **2008**, *38*, 71.
[12] R. S. Wray, *IBIS* **1887**, *29*, 420.
[13] H. Chen, P. Zhang, L. Zhang, H. Liu, Y. Jiang, D. Zhang, Z. Han, L. Jiang, *Nature* **2016**, *532*, 85.
[14] a) B. Hu, Z. Duan, B. Xu, K. Zhang, Z. Tang, C. Lu, M. He, L. Jiang, H. Liu, *J. Am. Chem. Soc.* **2020**, *142*, 6111; b) C. Li, H. Dai, C. Gao, T. Wang, Z. Dong, L. Jiang, *Proc. Natl. Acad. Sci. USA* **2019**, *116*, 12704.
[15] a) A. Tuteja A, W. Choi, M. Ma, J. M. Mabry, S. A. Mazzella, G. C. Rutledge, G. H. McKinley, R. E. Cohen, *Science* **2007**, *318*, 1618; b) J. Ou, G. Fang, W. Li, A. Amirfazli, *J. Phys. Chem. C* **2019**, *123*, 23976; c) T. Verho, C. Bower, P. Andrew, S. Franssila, O. Ikkala, R. H. A. Ras, *Adv. Mater.* **2011**, *23*, 673.
[16] a) J. F. Oliver, C. Huh, S. G. Mason, *J. Colloid Interface Sci.* **2015**, *59*, 568; b) J. Li, X. Zhou, J. Li, L. Che, J. Yao, G. McHale, M. K. Chaudhury, Z. Wang, *Sci. Adv.* **2017**, *3*, eaao3530.
[17] a) F. J. Higuera, A. Medina, A. Liñán, *Phys. Fluids* **2008**, *20*, 102102; b) A. Ponomarenko, D. Quéré, C. Clanet, *J. Fluid Mech.* **2011**, *666*, 146; c) P. Concus, R. Finn, *Proc. Natl. Acad. Sci. USA* **1969**, *63*, 292.
[18] F. Heslot, N. Fraysse, A. M. Cazabat, *Nature* **1989**, *338*, 640.

ADVANCED FUNCTIONAL MATERIALS

Supporting Information

for *Adv. Funct. Mater.,* DOI: 10.1002/adfm.202010634

Spontaneous Directional Self-Cleaning on the Feathers of the Aquatic Bird *Anser cygnoides domesticus* Induced by a Transient Superhydrophilicity

Kang Luan, Meijin He, Bojie Xu, Pengwei Wang, Jiajia Zhou, Binbin Hu, Lei Jiang, and Huan Liu**

Supporting Information

Spontaneous directional self-cleaning on the feathers of the aquatic bird *Anser cygnoides domesticus* induced by a transient superhydrophilicity

Kang Luan[#], Meijin He[#], Bojie Xu, Pengwei Wang, Jiajia Zhou, Binbin Hu*, Lei Jiang, Huan Liu**

Dr. K. Luan, Dr. M. He, Dr. B. Xu, Dr. P. Wang, Prof. J. Zhou, Prof. L. Jiang, Prof. H. Liu
Key Laboratory of Bio-Inspired Smart Interfacial Science and Technology of Ministry of Education, School of Chemistry, Beijing Advanced Innovation Center for Biomedical Engineering, Beihang University
Beijing 100191, P. R. China
E-mail: liuh@buaa.edu.cn
bojiexu@buaa.edu.cn
Dr. K. Luan, Prof. B. Hu
Key Laboratory for Special Functional Materials of Ministry of Education, National & Local Joint Engineering Research Center for High-efficiency Display and Lighting Technology, School of Materials Science and Engineering, Collaborative Innovation Center of Nano Functional Materials and Applications, Henan University
Kaifeng, 475001, P. R. China
E-mail: hbb@henu.edu.cn
Prof. L. Jiang
CAS Key Laboratory of Bio-inspired Materials and Interfacial Science, Technical Institute of Physics and Chemistry, Chinese Academy of Sciences
Beijing 100190, P. R. China

[#] These authors contributed equally

Supplementary Text 1: Theoretical analysis based on the minimization of a system's free energy.

In order to confirm that the high-surface-tension liquid is capable of replacing low-surface-tension liquid, the free energy of two systems where the textured feather was completely wetted by both high- and low-surface-tension liquids were calculated. Configuration A and B refer to the states where the fibrous feather is completely wetted by low surface tension liquid (A) and high surface tension liquid (B), respectively.

In order to find the condition that the energy state of the Configuration A is higher than the Configuration B, it must have E_A - E_B > 0, which can be further expressed as,

$$\Delta E = E_A - E_B = R(\gamma_{SA} - \gamma_{SB}) + \gamma_A - \gamma_B > 0 \qquad \text{(Equation S1)}$$

In particular, Supplementary Equation 1 is reduced to measurable quantities with the use of the Young equation (for example, Joanna Aizenberg *et al*., *Nature*, 2015, 519, 70), where we have,

$$\Delta E = R(\gamma_B \cos\theta_B - \gamma_A \cos\theta_A) + \gamma_A - \gamma_B > 0 \qquad \text{(Equation S2)}$$

Where γ_A and γ_B are the surface tensions for the liquid to be repelled and the infused liquid, respectively, γ_{SB} is the interfacial tension of the solid-liquid interface, θ_A and θ_B are the equilibrium CAs of the liquids on a flat feather, respectively. *R* represents the roughness factor of the feather, which is defined as the ratio between the actual and projected areas of the surface. The value of the roughness for the feather fiber is estimated to be 2 (Wong, T. S. *et al*., *Nature* 2011, 477, 443) and the calculation indicates that E_A - E_B > 0 is true, which is consistent with the experimental results. Moreover, we also made similar conclusion on the solidified PDMS surface: the liquid with high-surface-tension can drive off the liquid with low-surface-tension.

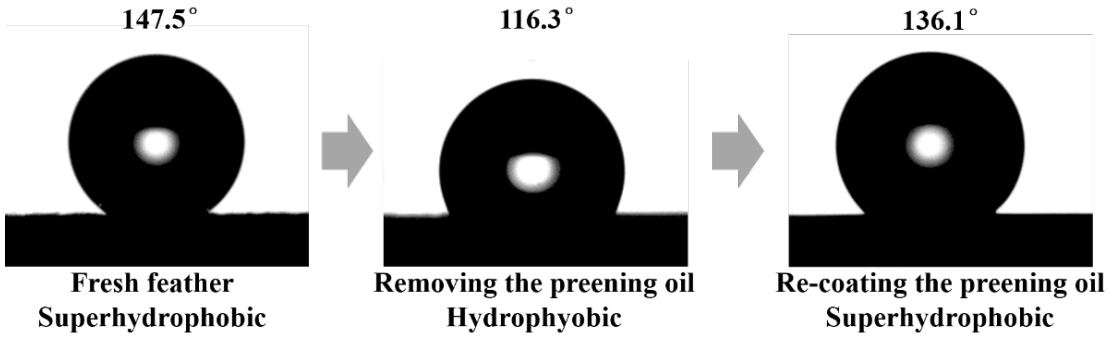

Figure S1. The water contact angle (WCA) on the feather with different treatment. The fresh feather shows high WCA of ca. 147.5°, exhibiting a typical superhydrophobic state. After removing the surface lipids by NaOH treatment, the WCA decreases drastically to ca. 116.3°, indicating a severely impaired superhydrophobicity. When the preening oil was artificially coated on the feather, the surface superhydrophobicity was recovered with a WCA of ca. 136.1°.

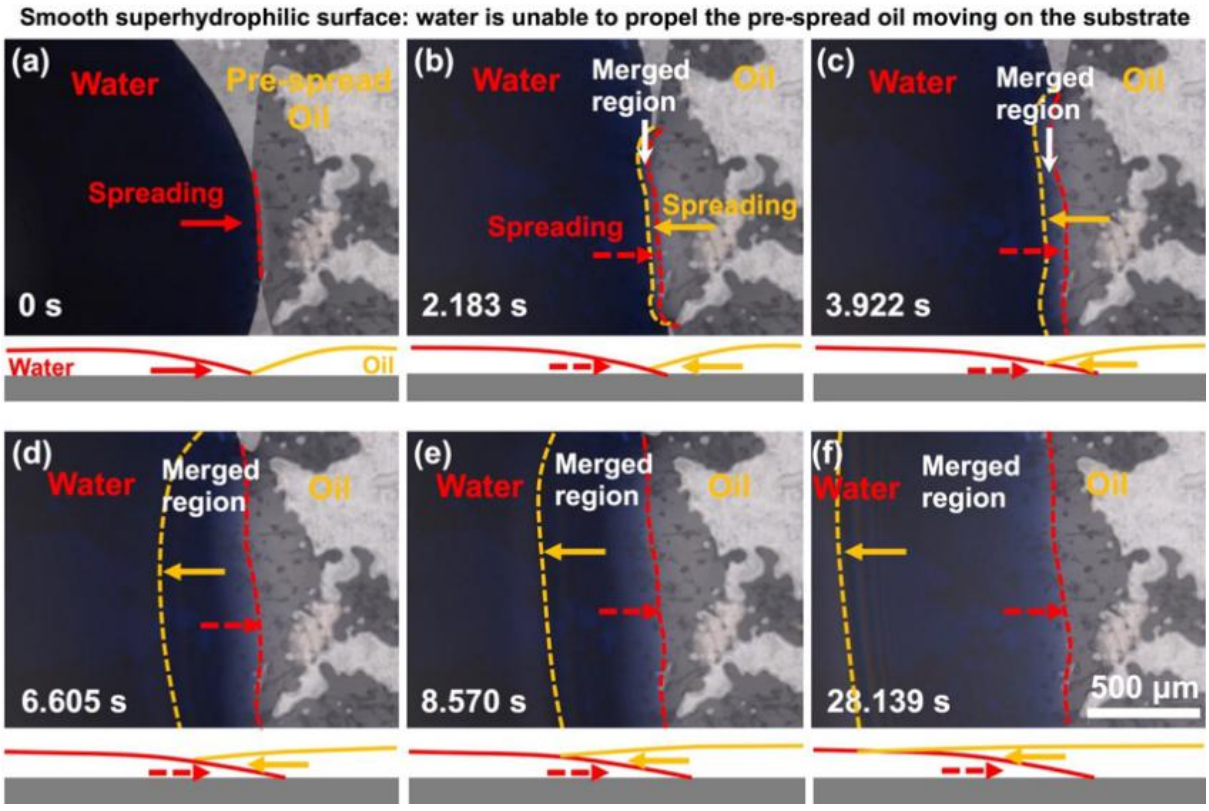

Figure S2. On a smooth superhydrophilic surface, the water and the pre-spread oil would merge together and form bilayer liquids, with no oil expulsion off the substrate in-plane.

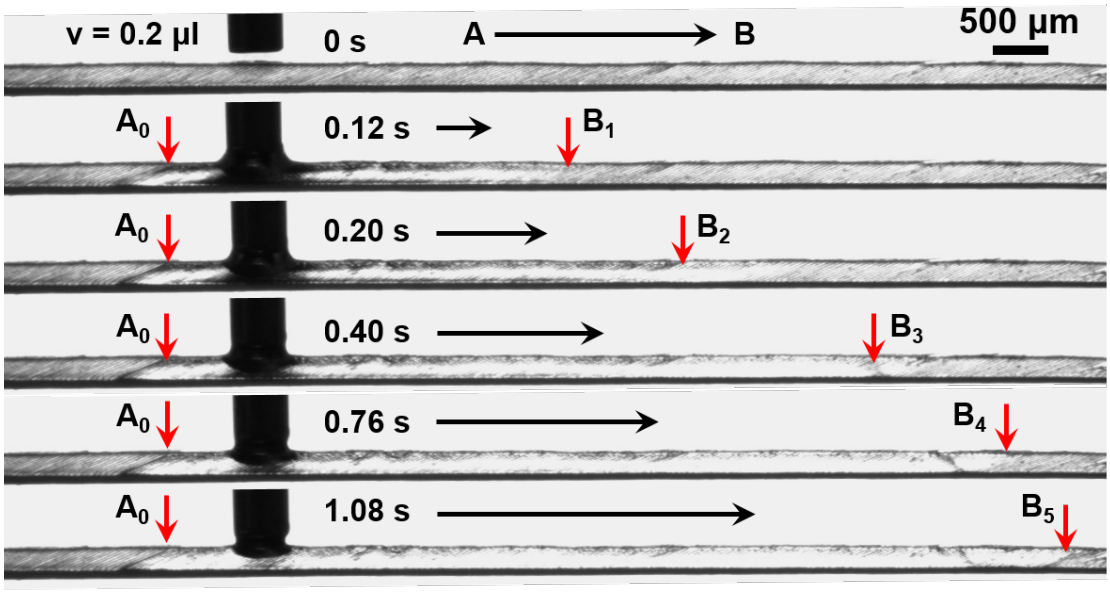

Figure S3. The directional transport of 1, 2-dichloromethane on the grooved barbules side with an average velocity of ~ 6.74 mm s^{-1} and an instantaneous fastest velocity of 23.37 mm s^{-1}.

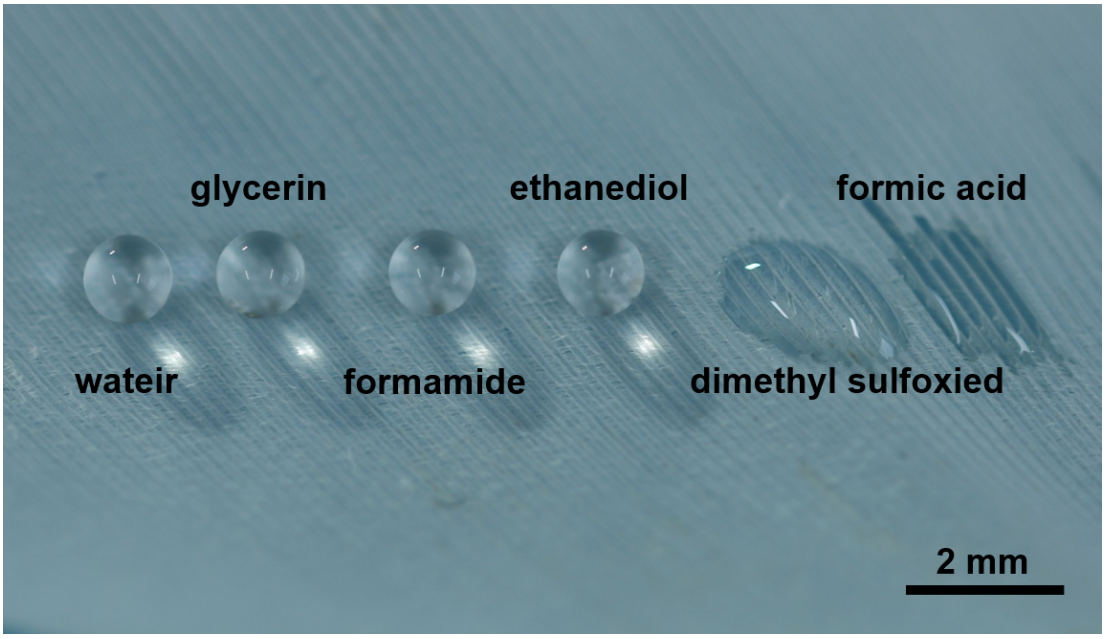

Figure S4. The status of liquid droplets with different surface tension on the natural feather. The surface tension of the liquid decrease successively from left to right. Particularly, dimethyl sulfoxide (43.6 dyn cm^{-1}) and formic acid (37.7 dyn cm^{-1}) can wet the feather without spreading.

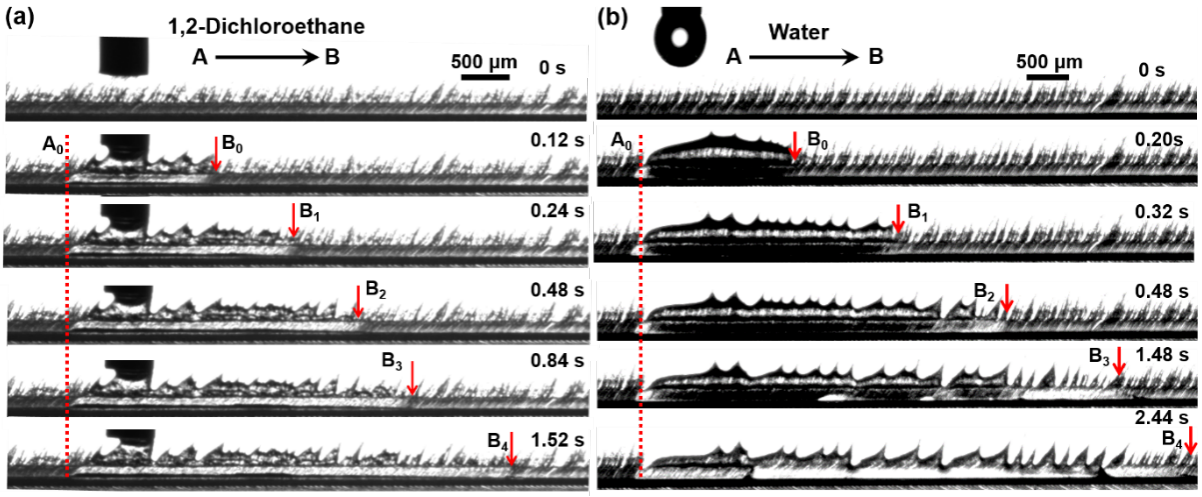

Figure S5. The directional transport of liquids with different surface tensions on the hooked barbules side of the feather. (a) the directional transport of 1, 2- dichloroethane (0.2 μl). (b) the directional transport of water (0.2 μl) in a rather fast velocity on a superhydrophilic feather.

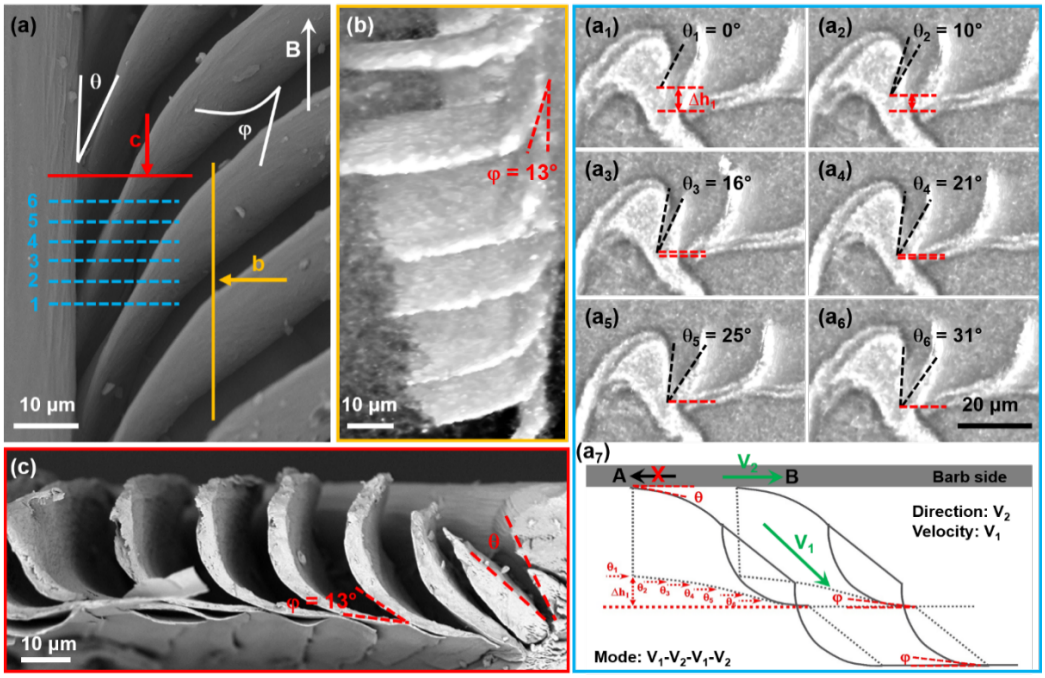

Figure S6. Micro-structure of the hooked barbules. (a, c) Micro-channels are formed by overlapped barbules, showing two kinds of wedge angle: the gradient angle θ and the fixed angle φ. The cross sections at different location of angle θ show that the value of angle θ increases from 0° to approximately 31° in direction *B*, as shown in a_1-a_6. The schematic cartoon of the microstructures of the hook barbules was shown in a_7. Typically, the opening end of angle θ is higher than the angle φ, and the $\Delta h'$ gradually decreases with the increase of the value of angle θ. (b) The side-view of hook barbules shows the tiny angle φ ca. 13°.

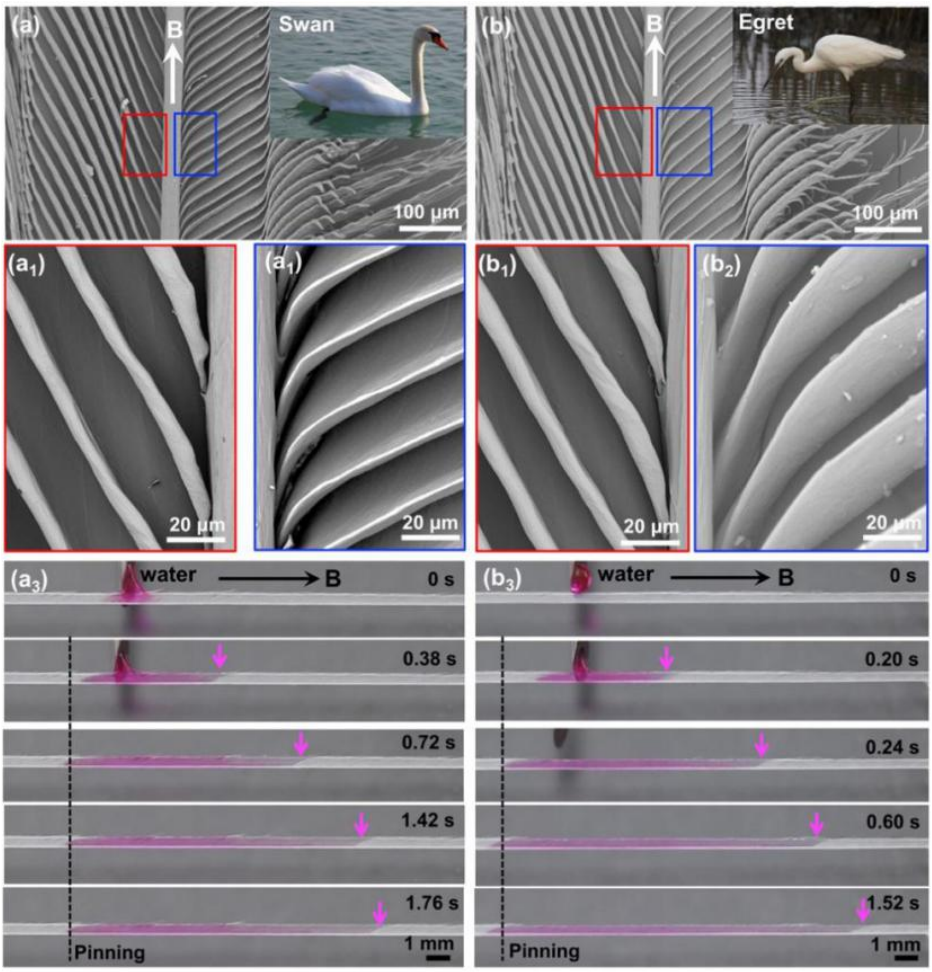

Figure S7. The micro-structures of the feather of the aquatic bird of (a) the swan *Cygnus cygnus* and (b) the egret *Egretta garzetta garzetta*, which show very similar structural characteristic with that of the goose feather. (a_3, b_3) After being wetted by their own saliva, the unique directional transport of water on it were observed on both feathers, by which the directional self-cleaning can be realized.

Movie S1.

The typical directional water transport on the grooved barbule side of the feather after being wetted by its saliva.

Movie S2.

Directional self-cleaning behavior on the superhydrophilic goose feather, where the water can easily drive away the pre-spread oil in a preferred direction.

Movie S3.

The cross section and 3D views of the feather obtained by X-ray micro-computed tomography.

Movie S4.

The directional water transport on both the bio-inspired artificial feather and the large-scale substrate (the water was stained into the red color).

Movie S5.

The directional self-cleaning on both the bio-inspired artificial feather and the large-scale substrate, where the oil contaminants (stained into the red color for easy observation) was driven away from the substrate in a preferred direction, as arrows indicated.

Movie S6.

The typical directional transport of 1.2-dichloroethane and water on the hooked barbule side of the goose feather after being wetted by its saliva.